



# Proton-controlled synthesis of red-emitting carbon dots and application for hematin detection in human erythrocytes

Yan Jun Ju<sup>1</sup> · Na Li<sup>1</sup> · Shi Gang Liu<sup>1</sup> · Jia Yu Liang<sup>1</sup> · Xin Gao<sup>1</sup> · Yu Zhu Fan<sup>1</sup> · Hong Qun Luo<sup>1</sup> · Nian Bing Li<sup>1</sup>

Received: 25 September 2018 / Revised: 20 November 2018 / Accepted: 10 December 2018 / Published online: 7 January 2019  
© Springer-Verlag GmbH Germany, part of Springer Nature 2019

## Abstract

The Red-emitting nitrogen-doped carbon dots (N-CDs) are synthesized using o-phenylenediamine by a one-step method, and can serve as a fluorescent probe for “turn off” detection of hematin in human red cells. The red-emitting N-CDs can be obtained only in acidic conditions and the emission of the red-emitting N-CDs is pH-dependent, indicating proton-controlled synthesis and emission. The red-emitting N-CDs are 2.7 nm in mean size and have a uniform dispersion and exhibit a high quantum yield (12.8%) and great optical properties. The developed sensing system for hematin displays a linear response from 0.4 to 32  $\mu\text{M}$  with a detection limit of 0.18  $\mu\text{M}$ . Importantly, this fluorescent probe demonstrates a good potential practicability for the quantitative detection of hematin in complex matrixes.

**Keywords** N-Doped carbon dots · Red emission · Proton-controlled synthesis · Hematin detection · Human erythrocytes

## Introduction

Carbon dots (CDs) attract tremendous attentions in recent years due to their remarkable advantages such as great optical properties, excellent biocompatibility, and good water solubility [1, 2]. Consequently, CDs have been found wide utilization in many fields, such as sensing, optical imaging, and cell labeling [3–7]. Recently, many prepared methods are developed to adjust the optical properties of CDs. Mainly blue- to green-fluorescent CDs have been synthesized [2, 5–8]. But some defects limit their further applications, especially in optoelectronic devices and biomedical applications due to severe photodamage of ultraviolet excitation light and obvious blue autofluorescence of biological matrix. In the meantime, red light exhibits excellent tissue osmotic performance.

Moreover, red fluorescent CDs can provide vital components for full-color emitting; thus, red CDs are very suitable for biomedical application. To the best of our knowledge, nevertheless, very few simple and reproducible synthetic methods for red emissive CDs are reported [9, 10]. Therefore, it is important to find efficient and easy prepared pathways for red fluorescent CDs.

Hematin (Fe(III) protoporphyrin IX with a hydroxyl group ( $\text{OH}^-$ ) ligand) is derived from the oxidized form of heme (Fe(II)-protoporphyrin IX), which is the main prosthetic group of proteins such as myoglobin and hemoglobin [11]. A hemoglobin molecule has four hemes, which exist on each of the hemoglobin subchains. After the autoxidation of hemoglobin to methemoglobin, the Fe(II) is oxidized to Fe(III), which binds an  $\text{OH}^-$ . Thereafter, heme is freed from hemoglobin to red cells as hematin [12, 13].

Hematin has been testified as a kind of toxic substance. Firstly, it is a forceful hemolytic agent and can trigger lyses of human red cells and other type of cells [14–16]. Secondly, hematin can cause membrane damage by generating reactive oxygen species (ROS) including hydroxyl radicals, superoxide radicals, and  $\text{H}_2\text{O}_2$ , which can mediate lipid peroxidation [17, 18]. Moreover, the levels of hematin would become abnormal under pathological condition and result in diverse inflammatory diseases, such as immune-mediated disorders, renal insufficiency, and vascular disease [19, 20]. Considering the adverse impact of hematin on human body, it is very

**Electronic supplementary material** The online version of this article (<https://doi.org/10.1007/s00216-018-1547-z>) contains supplementary material, which is available to authorized users.

✉ Hong Qun Luo  
luohq@swu.edu.cn

✉ Nian Bing Li  
linb@swu.edu.cn

<sup>1</sup> Key Laboratory of Eco-environments in Three Gorges Reservoir Region (Ministry of Education), School of Chemistry and Chemical Engineering, Southwest University, Chongqing 400715, China

significant to develop a fast, efficient, and reliable method for determination of hematin. However, there is a paucity of the literature about determination of hematin in erythrocytes.

Most reports for heme quantification mainly are centered on detecting the total heme in red cells, including the free heme and heme-containing protein, such as hemoglobin and myoglobin. Colorimetry [21], high-performance liquid chromatography (HPLC) [22], and mass spectrometry [23] were used in some reports. But these works do not provide a way to directly detect hematin in red cells. Thus, the detection of hematin in erythrocytes is still a great challenge. To realize the goal of detecting hematin directly, researchers have focused on developing new strategies in recent years. According to the adsorption properties of hematin, Liu et al. [24] reported an approach for detecting hematin in human red cells. But hematin must be separated from bulk hemoglobin firstly, which makes the pretreatment process complicated and time-consuming. Due to their low toxicity, high photostability, great water solubility, and good biocompatibility, carbon dots were successfully applied to many analytical detection fields as fluorescent probes [25, 26]. Boron-doped graphene quantum dots (BGQDs) were used to test the hematin content in red cells without the separation of hematin from hemoglobin [27]. But the preparation process of BGQDs is tedious, needing careful control of the preparation conditions.

In this work, the strong red emissive nitrogen-doped carbon dots (N-CDs) were synthesized using a hydrothermal carbonization method. Scheme 1 exhibits that the preparation process of N-CDs is convenient. Since *o*-phenylenediamine is rich in carbon and amino groups, it can be used as nitrogen and carbon sources to synthesize N-CDs without further surface modification or conjugation.

The fluorescence intensity of the N-CDs decreased with addition of hematin. Meanwhile, the N-CDs were successfully applied to directly detecting hematin in human red cells without separating hematin from hemoglobin, which exhibits a potential application of this method for determination of hematin in complex biological samples.

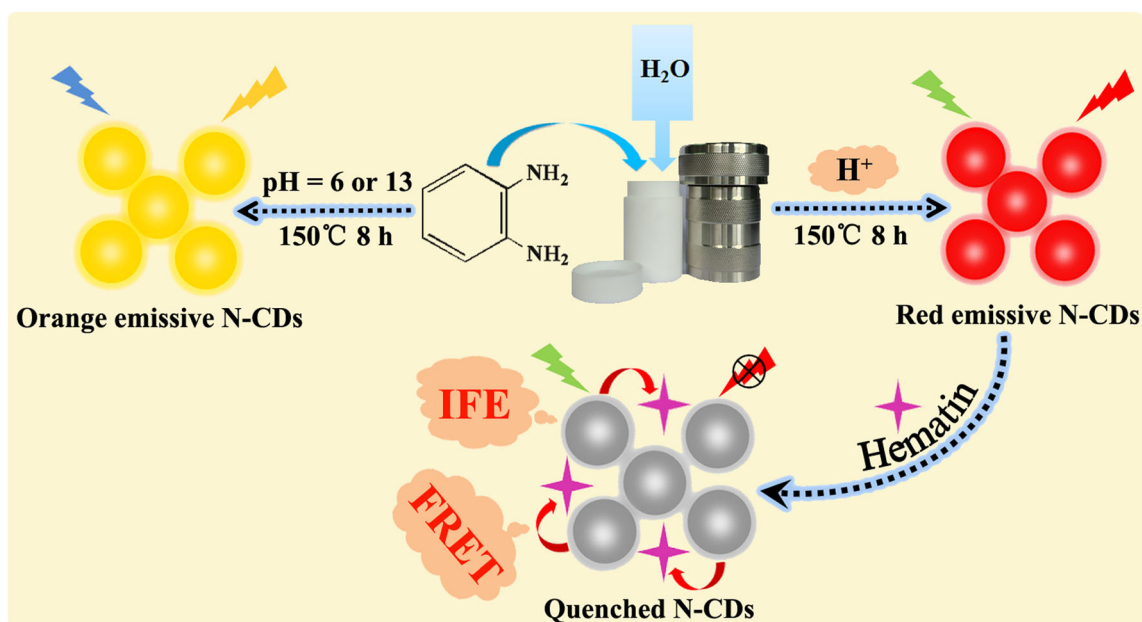
## Materials and methods

### Reagents and materials

HCl, *o*-phenylenediamine (oPD), HNO<sub>3</sub>, H<sub>2</sub>SO<sub>4</sub>, tetra-*n*-butylammonium hexafluorophosphate (Bu<sub>4</sub>NPF<sub>6</sub>), sodium chloride (NaCl), *m*-phenylenediamine (mPD), and *p*-phenylenediamine (pPD) were supplied by Aladdin Reagent Co., Ltd. (Shanghai, China). A Britton–Robinson (BR) buffer was prepared for controlling the acidity.

### Apparatus

The high-resolution transmission electron microscopy (HRTEM) data of N-CDs were performed on a JEM-2100 electron microscope (JEOL Ltd., Japan). X-ray photoelectron spectroscopy (XPS) spectra were collected by an ESCALab 250Xi (Thermo Fisher Scientific, USA). The Fourier transform infrared (FTIR) spectra were collected using a Bruker IFS 113v spectrometer (Bruker, Germany). The fluorescence lifetime was measured with an FLSP920 fluorescence spectrometer (Edinburgh, UK). The UV-vis absorption spectra were gained from a UV-Vis 2450 spectrophotometer (Suzhou Shimadzu Instrument Co., Ltd., China). The



**Scheme 1** Schematic diagram showing the synthetic strategy of N-CDs and detection principle for hematin

electrochemical measurement was performed on a CHI660 electrochemical station (Shanghai CHI Instruments Co., Ltd., China). A common three-electrode cell was used, including the Ag/AgCl (sat.KCl) reference electrode, and two Pt wire electrodes as the counter electrode and the working electrode, respectively. The fluorescence spectra were recorded with an F-4500 fluorescence spectrophotometer (Hitachi Ltd., Japan).

### Synthesis of red-emitting N-CDs

The red-emissive N-CDs were prepared by a carbonation method according to a previous report with some modifications [28]. Briefly, 27 mg of oPD and 50  $\mu$ L of HCl (1 M) were added to 5 mL of ultrapure water. And the solutions were heated at 150  $^{\circ}$ C for 8 h in a tetrafluoroethylene autoclave (25 mL). After cooling to room temperature, the deep red products were centrifuged at 12,000 rpm for 25 min, and then the sediment was removed. And the product was collected for further use. Furthermore, other control carbon dots were prepared in the same conditions except that oPD was replaced by mPD and pPD, and HCl was replaced by HNO<sub>3</sub> and H<sub>2</sub>SO<sub>4</sub>, respectively.

### Fluorescence quantum yield assay

By using rhodamine B with QY = 89% as a reference, the relative quantum yield (QY) of N-CDs was estimated (see Electronic Supplementary Material (ESM) Fig. S1). And the N-CDs and rhodamine B were dissolved in ultrapure water (refractive index of 1.33) and absolute ethyl alcohol (refractive index of 1.36), respectively, and their absorbance were kept less than 0.05 at 560 nm to avoid self-absorption mechanism.

The quantum yield was estimated by the equation below:

$$\varphi_x = \varphi_{st} \left( \frac{Grad_x}{Grad_{st}} \right) \left( \frac{\eta_x}{\eta_{st}} \right)^2 \quad (1)$$

where  $\varphi$  represents the QY,  $\eta$  denotes the refractive index, and *Grad* is the slope of curve. And the subscript “x” represents the N-CDs samples and “st” represents the standard. And  $\eta_x / \eta_{st} = 0.98$ .

### Detection of hematin by red-emitting N-CDs

For detecting hematin, 10  $\mu$ L of N-CDs (10 mg/mL), 20  $\mu$ L of various concentrations of hematin, and 470  $\mu$ L of BR buffer (pH 3.2) were mixed together. After a few minutes, the fluorescence signals were recorded on the spectrofluorophotometer at the excitation wavelength ( $\lambda_{ex} = 560$  nm).

### Preparation of hemolysate

Blood sample was provided by healthy adults from our laboratories. We prepared the hemolysate based on a reported method [27]. A portion of 20 mL of isotonic 0.9% NaCl solutions was added to 2 mL of blood samples. The suspension was then uniformly mixed by gently agitating the tube. Next, to remove the supernatant, the mixture was centrifuged at 3000 rpm for 10 min. After washing three times by repeating the above process, the sediment was dispersed in 25 mL of ultrapure water. Due to different osmotic pressures between the water and the red cells, the red cells ruptured. To compress the cell membranes, the suspension was centrifuged at 10,000 rpm. Finally, the hemolysates were obtained and stored at 4  $^{\circ}$ C for further use. The hemolysates were diluted 100-fold using ultrapure water before use.

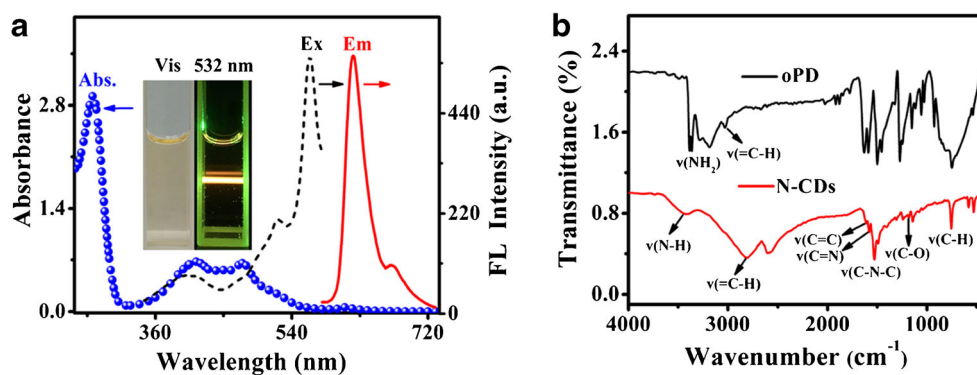
## Results and discussion

### Proton-controlled synthesis of red-emitting N-CDs

o-Phenylenediamine was used as a precursor to prepare N-CDs. We adjusted the pH of the reaction system with HCl or NaOH in the preparation process of the N-CDs. Interestingly, red-emitting N-CDs were obtained under acidic condition, whereas the N-CDs synthesized in neutral and alkaline conditions emitted orange fluorescence (see ESM Fig. S2A). The results indicate that pH value of reaction system acts as a significant factor in the preparation of N-CDs with different emissions. A previous report claimed that HNO<sub>3</sub> played a significant role to the red emission of N-CDs [29]. To prove the fact that different emissions are caused by pH rather than by a specific acid, we replaced HCl with HNO<sub>3</sub> or H<sub>2</sub>SO<sub>4</sub>. As shown in Fig. S2B (see ESM), all N-CDs prepared by adding various acids show red fluorescence, illustrating that the acid source has no influence on the formation of the red-emitting N-CDs and the proton takes an important role to the red emission. Furthermore, when HCl was added, the as-prepared orange-emitting N-CDs have no redshift in the emission wavelength (see ESM Fig. S2C), demonstrating that the proton has an important influence upon the synthesis of red-emitting N-CDs. In addition, we used mPD and pPD to synthesize N-CDs at the same conditions. The prepared N-CDs using mPD and pPD show the fluorescence emission peaks at 510 and 600 nm, respectively, having a blueshift compared to that with oPD, and their fluorescence intensities are lower than those of the N-CDs synthesized by oPD (see ESM Fig. S3). Therefore, oPD was selected to obtain red-emitting N-CDs finally.

Next, the optical property of the red-emitting N-CDs was studied. The UV-vis absorption spectrum of the N-CDs (Fig. 1a) displays a strong absorption peak at 277 nm and two weak absorption bands at 413 and 475 nm in the range

**Fig. 1** **a** UV-vis absorption spectrum (Abs) and fluorescence spectrum of N-CDs. Insets display pictures of N-CDs under natural light (left) and laser pointer at 532 nm (right). **b** FTIR spectra of oPD and N-CDs. Conditions: N-CDs, 0.2 mg/mL; BR buffer, pH 3.2



of 410–630 nm because of the  $\pi$ - $\pi^*$  transition of C=C bond, and  $n$ - $\pi^*$  transitions of C=N and C=O bonds, respectively [28, 30]. The N-CDs reveal a remarkable fluorescence peak at 620 nm and a shoulder at 675 nm when excited at 560 nm. Furthermore, the solution emits strong red fluorescence radiated with a laser pointer of 532 nm, and the N-CDs solutions are pale yellow (insets of Fig. 1a). The N-CDs exhibit an obvious excitation-independent emission characteristic (see ESM Fig. S4), which is attributed to uniform microstructure and surface chemical state of the N-CDs [31]. The QY of the N-CDs was 12.8% at excitation of 560 nm, using rhodamine B as a reference (see ESM Fig. S1). The functional groups on N-CDs were explored by using the FTIR spectroscopy. As illustrated in Fig. 1b, the amino groups of oPD (3386–3185  $\text{cm}^{-1}$ ) are transformed to secondary amine groups of N-CDs (3419  $\text{cm}^{-1}$ ). Furthermore, the stretching vibration of =C–H at 3030  $\text{cm}^{-1}$  has a significant enhancement and shifts to lower wave at 2809  $\text{cm}^{-1}$  from oPD to N-CDs, suggesting the prepared N-CDs with larger conjugated degree. The obvious characteristic bands at 1529, 1580, and 1610  $\text{cm}^{-1}$  are attributed to C–N–C, C=N, and C=C, respectively. The stretching vibration of C–H of aromatic benzene with the phenazine skeletons is situated at 755 and 608  $\text{cm}^{-1}$ . The above analysis testified the presence of phenazine and imine structures in the N-CDs [29, 32–34].

Figure 2a exhibits TEM image of the red-emitting N-CDs, which exhibits that the particles are nearly spherical and monodispersed. Moreover, the N-CDs have a small size distribution (2.0–3.5 nm) with a mean diameter of 2.7 nm. The inset of Fig. 2a shows distinct lattice spacing (0.20 nm) in the HRTEM image, which can be ascribed to (100) facet of graphitic carbon [35]. The XPS spectra were used to further study the structures and elemental composition on the surface of the red-emitting N-CDs. The full spectrum (Fig. 2b) displays that the N-CDs consisted mostly of carbon (C), oxygen (O), and nitrogen (N). Figure 2c shows the C1s analysis reveals four different peaks at 284.4 (C–C/C=C), 284.9 (C–N), 285.9 (C–O), and 287.0 eV (C=N) [29, 36]. Moreover, the N1s spectrum (Fig. 2d) exhibits these peaks at 398.8, 399.9, and 401.1 eV corresponding to pyridinic N, pyrrolic N, and amino N, respectively [37, 38].

### Proton-mediated emission of red-emitting N-CDs

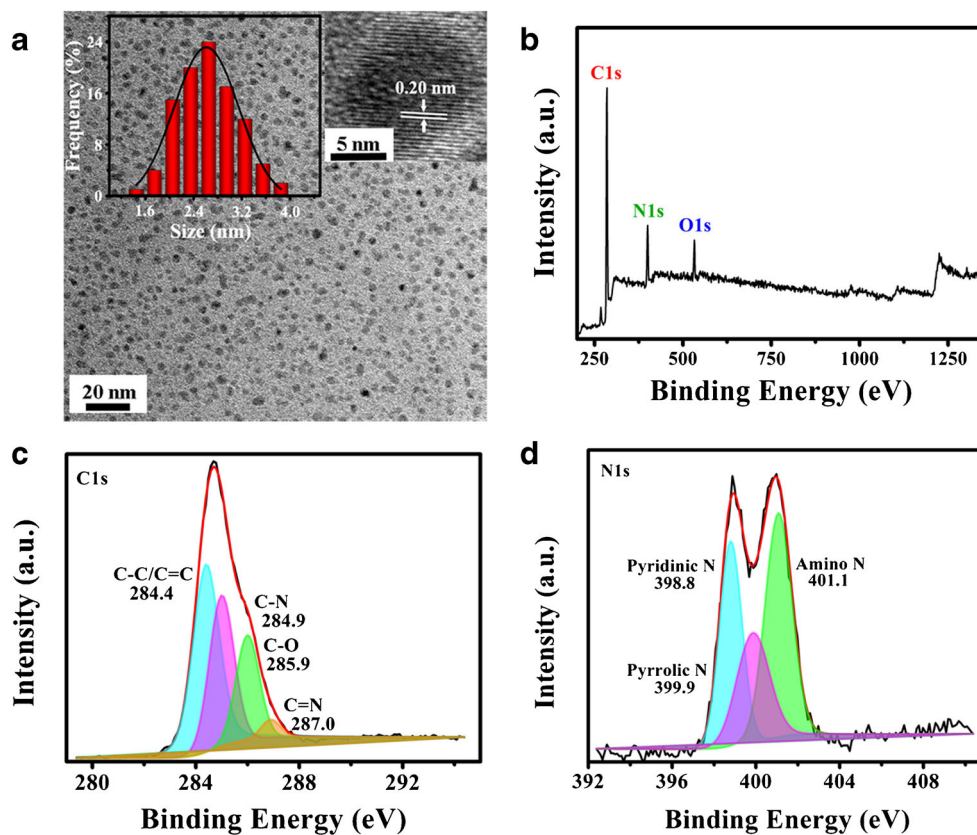
It can be seen that the fluorescence of the red-emitting N-CDs was pH-dependent. Figure 3a exhibits the fluorescence variation of the N-CDs with different pH values (1.8–5.0). It is also found that although there is no shift of emission wavelength, the fluorescence intensity of the N-CDs is decreased with raising pH and has a good linear relationship to pH (1.8–5.0) (Fig. 3b). The fluorescence of the N-CDs exhibits a good reversibility against pH by repeating three-time measurements (the inset of Fig. 3b). The above results imply that a stable and reversible sensing system for pH assay can be established using the red-emitting N-CDs.

The response of the red-emitting N-CDs toward pH might be ascribed to protonation and deprotonation of the nitrogen doping in the rigid carbon skeleton structures [39]. In acidic condition, the surface groups of N-CDs and the N in the rigid carbon skeleton were protonated. With increasing pH value, the doped nitrogen in N-CDs was deprotonated firstly, influencing the  $\text{sp}^2$  domain of the N-CDs [35]. Thus, the fluorescence of N-CDs was quenched gradually. In order to verify this inference, the fluorescence spectra and zeta potentials of N-CDs with different pH values (1.8–5.0) were measured. Figure 3b exhibits that the fluorescence intensity of N-CDs decreased greatly at pH 5.0, which indicated that the surface groups were deprotonated. Furthermore, with increasing pH, the zeta potential of the N-CDs was more negative (see ESM Fig. S5), further testifying the deprotonation process.

### Stability of the red-emitting N-CDs

The stability of the synthesized red-emitting N-CDs was explored. Figure S6A (see ESM) exhibits the N-CDs can be stored at 4 °C for at least 2 months, which still kept stable without obvious decrease in fluorescence. Moreover, the sign of photobleaching was not found for the N-CDs under continuous irradiation for 1 h by a UV lamp of 365 nm (see ESM Fig. S6B). As shown in Fig. S7A (see ESM), the fluorescence intensity of the N-CDs is stable for at least 30 min in different pH solutions (pH 2.5, 3.5, and 4.5). In addition, the

**Fig. 2** **a** TEM of N-CDs. Inset to **a**: HRTEM and histogram of the size distribution of N-CDs. **b** XPS survey spectrum of N-CDs. High-resolution XPS spectra of **c** C1s and **d** N1s of N-CDs



fluorescence of the N-CDs can still remain constant even in the solution with high ionic strength (100 mM NaCl, see ESM Fig. S7B). From the above descriptions, the as-prepared N-CDs have good stability even under extreme conditions, which makes them possess good potential for hematin detection in biological samples.

### Establishment of sensing system for hematin with red-emitting N-CDs

The red-emitting N-CDs reveal intrinsic fluorescence, abundant surface groups, and excellent water solubility, indicating their good application prospect in chemical and biological fields. In this work, the fluorescence of red-emitting N-CDs

decreased with addition of hematin. The effect of pH on the system for detecting hematin was investigated in the BR buffer by monitoring the change of the fluorescence intensity ratio,  $(F_0 - F) / F_0$ , where  $F_0$  and  $F$  denote the fluorescence intensity of N-CDs before and after addition of hematin, respectively. Figure S8A (see ESM) shows that in the pH range of 2.6–4.5,  $(F_0 - F) / F_0$  does not obviously change. Considering the sensitivity of detection and buffer capacity of the buffer, the pH 3.2 BR buffer was chosen for the experiments. Figure 4a reveals the fluorescence quenching of N-CDs by different concentrations of hematin (0–35  $\mu\text{M}$ ), which suggests that the hematin sensing system can be established using N-CDs. And Fig. 4b indicates a relationship of  $(F_0 - F) / F_0$  to the hematin concentration. The inset of Fig. 4b exhibits the

**Fig. 3** **a** Fluorescence spectra of N-CDs in the BR buffers with different pH values (from 1.8 to 5.0). **b** Linear relationship of the fluorescence intensity of N-CDs versus pH value. The inset is the reversibility of fluorescence toward pH between 1.8 and 5.0. Conditions: N-CDs, 0.2 mg/mL

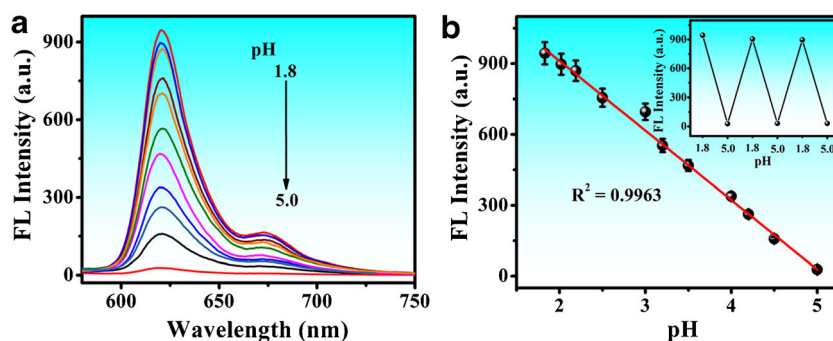
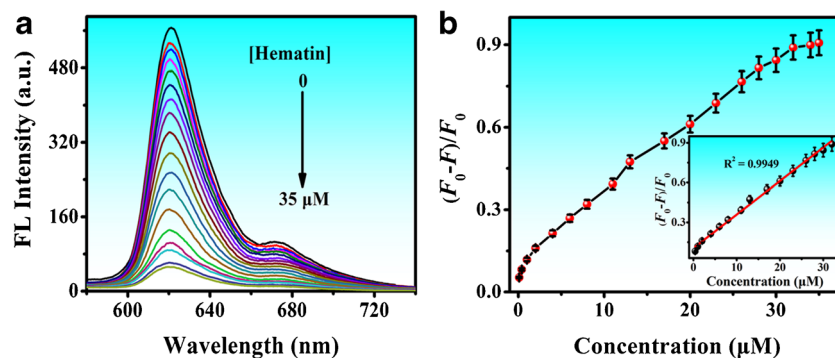


**Fig. 4** **a** Fluorescence spectra of N-CDs with addition of different concentrations of hematin. **b** Relationship between  $(F_0 - F)/F_0$  and the hematin concentrations from 0 to 35  $\mu\text{M}$  ( $F_0$  and  $F$  are the fluorescence intensity of N-CDs in the absence and presence of hematin, respectively). And the inset exhibits the linear relationship for hematin in the 0.4–32  $\mu\text{M}$  range. Conditions: N-CDs, 0.2 mg/mL



intensity ratio displays a linear relationship against hematin concentration from 0.4 to 32  $\mu\text{M}$  with the regression equation of  $(F_0 - F)/F_0 = 0.025C + 0.106$ , where  $C$  represents concentration of hematin. The detection limit (defined as  $3\sigma/\text{slope}$ ) for hematin was 0.18  $\mu\text{M}$ . Moreover, the influence of the incubation time on the intensity ratio was explored. After adding hematin for 30 s, the fluorescence can be quenched and keep stable for 20 min (see ESM Fig. S8B), suggesting that the N-CDs interact with hematin quickly. Therefore, the as-synthesized N-CDs can be used for real-time tracking hematin in real samples. In addition, the fluorescence change of orange-emitting N-CDs with adding hematin (0–35  $\mu\text{M}$ ) was explored (see ESM Fig. S9A). And Fig. S9B (see ESM) shows a linear relationship of  $(F_0 - F)/F_0$  to the hematin concentration (4–20  $\mu\text{M}$ ) with a linear correlation ( $R^2 = 0.9941$ ). The detection limit (defined as  $3\sigma/\text{slope}$ ) for hematin is 1.43  $\mu\text{M}$ . As a result, it can be seen that the analysis method established by red-emitting N-CDs is more sensitive and has a wider linear range for hematin. Meanwhile, a comparison with the previous reports for hematin detection is summarized (see ESM Table S1). It can be seen that our method is rapid and reliable. Importantly, our sensing system has several remarkable merits including simple synthesis and great sensitivity for hematin detection.

### Selectivity study for hematin detection

For investigating the selectivity of this probe to hematin, the fluorescence signals of N-CDs were explored with some biological molecules (hemoglobin (Hb), glutathione (GSH), uridine (Uri), adenosine (Ade), L-cysteine (L-Cys), glucose (Glu), ascorbic acid (AA), and L-arginine (L-Arg)) and metal ions ( $\text{Li}^+$ ,  $\text{Na}^+$ ,  $\text{K}^+$ ,  $\text{Zn}^{2+}$ ,  $\text{Al}^{3+}$ , and  $\text{Fe}^{3+}$ ). Figure 5 displays that the fluorescence of the N-CDs has an obvious decrease when adding hematin, whereas these biological substances and metal ions exhibit an insignificant fluorescence quenching ability to N-CDs, which suggests that the N-CDs exhibit remarkable selectivity for hematin over other coexisting biological substances possibly. Therefore, the results reveal that the established system can be reliable and selective determination of hematin in complex biological samples.

### Mechanism of hematin-induced quenching

To understand the fluorescence quenching mechanism of N-CDs by hematin, some experiments have been performed. The fluorescence emission spectrum of N-CDs shows broad overlap with the absorption spectrum of hematin (Fig. 6a). Also, we measured the fluorescence lifetime of N-CDs and found it to be 0.666 ns (Fig. 6b), but when added 10 and 20  $\mu\text{M}$  hematin, the fluorescence lifetimes were 0.645 and 0.585 ns, respectively. Hence, the fluorescence quenching might be caused by fluorescence resonance energy transfer (FRET) [40]. Moreover, the zeta potential of N-CDs was 8.88 mV in the BR buffer (pH 3.2) (see ESM Fig. S5), but the zeta potential was increased to 11.47 mV with the addition of hematin, indicating that there is a strong interaction between the N-CDs and hematin. A close proximity between N-CDs and hematin makes FRET possible, which further confirms the possibility of quenching process via FRET.

To further give an insight on the quenching mechanism, the electrochemical properties of the N-CDs system were investigated using the cyclic voltammetry (CV). The energy levels of highest occupied molecular orbital (HOMO) and lowest

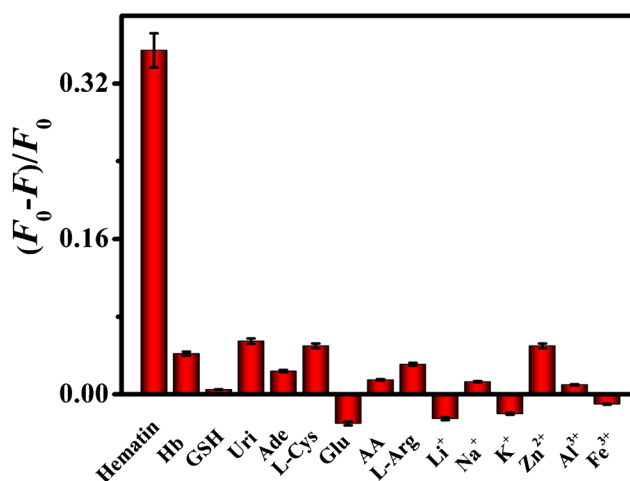
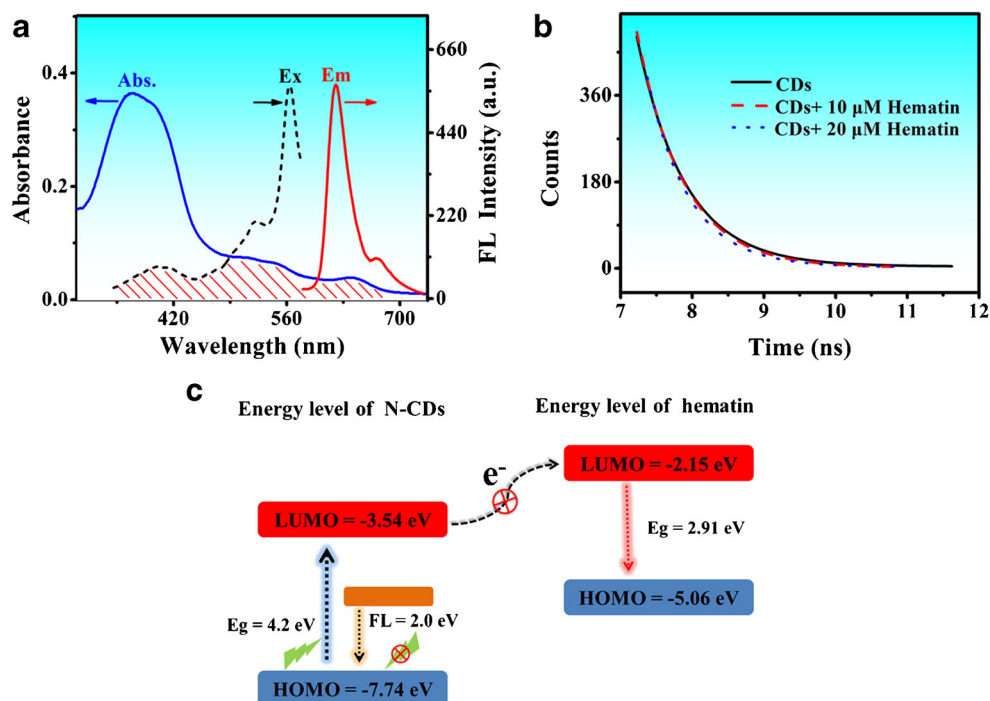


**Fig. 5** Fluorescence response of N-CDs with adding various analytes. The concentration of hematin is 10  $\mu\text{M}$ . And the concentration of other foreign substances is 50  $\mu\text{M}$ , except that Hb is 50 mg/mL. Conditions: N-CDs, 0.2 mg/mL

**Fig. 6** **a** UV-vis absorption spectrum of hematin (10  $\mu\text{M}$ ) and fluorescence spectra of N-CDs. **b** Time-resolved decay of N-CDs before and after adding 10 and 20  $\mu\text{M}$  hematin. **c** The  $E_{\text{HOMO}}$  and  $E_{\text{LUMO}}$  of N-CDs and hematin. Conditions: N-CDs, 0.2 mg/mL



unoccupied molecular orbital (LUMO) of N-CDs were measured, and Fig. S10 (see ESM) illustrates the detailed calculation process. The  $E_{\text{HOMO}}$  and  $E_{\text{LUMO}}$  of N-CDs are calculated as  $-7.74$  and  $-3.54$  eV, respectively, based on a reported method [41]. Moreover, the  $E_{\text{HOMO}}$  and  $E_{\text{LUMO}}$  of hematin are  $-5.06$  and  $-2.15$  eV, respectively, according to a previous report [27]. Figure 6c shows the electron transfer from the LUMO of the N-CDs to that of hematin cannot occur. The above results demonstrate that the ET quenching mechanism can be excluded.

In addition, the fluorescence excitation spectrum of N-CDs has a broad overlap with the absorption spectrum of hematin, suggesting the existence of inner filter effect (IFE)–caused quenching [2, 41]. Based on the above discussion, the possible quenching mechanism of the red-emitting N-CDs caused by hematin can be ascribed to FRET and IFE.

### Detection of hematin in red cell hemolysates

The N-CDs were used for detecting hematin in healthy human red cell hemolysates to explore the practicality of our method. We measured the samples that were spiked with standard hematin solution (0, 2, 4, 8  $\mu\text{M}$ ). The recoveries of these samples varied from 99.0 to 108.0% (see ESM Table S2) and the relative standard deviations (RSD) were below 3.77%, which shows a good repeatability of the method. Therefore, the sensing system exhibits a potential application for the reliable and selective hematin determination in human red cell samples.

### Conclusions

The red fluorescent N-CDs have been prepared successfully with o-phenylenediamine as a precursor using a one-step method. And the red-emitting N-CDs can be synthesized only in an acidic condition. Meanwhile, the emission of the red-emissive N-CDs was also pH-dependent, indicating a proton-controlled synthesis and emission of the red-emitting N-CDs. The red-emitting N-CDs can serve as a probe for quick and dependable determination of hematin without extracting hematin from hemoglobin in human erythrocytes. The developed sensing system for hematin displays a range of linear response of 0.4–32  $\mu\text{M}$  with the detection limit of 0.18  $\mu\text{M}$ . Hence, this fluorescence probe can be applied to monitor the concentration change of hematin in complex matrixes successfully, suggesting its dependable and broad application prospect for the low-cost, and fast diagnosis of hematin-induced disease.

**Funding information** This study received financial support from the National Natural Science Foundation of China (No. 21675131) and the Innovation Foundation of Chongqing City for Postgraduate (CYB 16053).

### Compliance with ethical standards

The study was approved by the Ethics Committee of Southwest University, and written informed consent was obtained from all individuals participating in the study prior to the collection of the human blood samples.

**Conflict of interest** The authors declare that they have no competing interests.

**Publisher's Note** Springer Nature remains neutral with regard to jurisdictional claims in published maps and institutional affiliations.

## References

- Wei L, Ma Y, Shi X, Wang Y, Su X, Yu C, et al. Living cell intracellular temperature imaging with biocompatible dye-conjugated carbon dots. *J Mater Chem B*. 2017;5:3383–90.
- Fan YZ, Zhang Y, Li N, Liu SG, Liu T, Li NB, et al. A facile synthesis of water-soluble carbon dots as a label-free fluorescent probe for rapid, selective and sensitive detection of picric acid. *Sensors Actuators B Chem*. 2017;240:949–55.
- Yang ST, Cao L, Luo PG, Lu F, Wang X, Wang HF, et al. Carbon dots for optical imaging in vivo. *J Am Chem Soc*. 2009;131:11308–9.
- Gao X, Ding CQ, Zhu AW, Tian Y. Carbon-dot-based ratiometric fluorescent probe for imaging and biosensing of superoxide anion in live cells. *Anal Chem*. 2014;86:7071–8.
- Gong X, Li Z, Hu Q, Zhou R, Shuang S, Dong C. N,S,P co-doped carbon nanodot fabricated from waste microorganism and its application for label-free recognition of manganese (VII) and l-ascorbic acid and AND logic gate operation. *ACS Appl Mater Interfaces*. 2017;9:38761–72.
- Li BL, Setyawati MI, Zou HL, Dong JX, Luo HQ, Li NB, et al. Emerging oD transition-metal dichalcogenides for sensors, biomedicine, and clean energy. *Small*. 2017;13:1700527.
- Ma Y, Zhang Z, Xu Y, Ma M, Chen B, Wei L, et al. A bright carbon-dot-based fluorescent probe for selective and sensitive detection of mercury ions. *Talanta*. 2016;161:476–81.
- Zhou J, Yang Y, Zhang CY. A low-temperature solid-phase method to synthesize highly fluorescent carbon nitride dots with tunable emission. *Chem Commun*. 2013;49:8605–7.
- Sun S, Zhang L, Jiang K, Wu A, Lin H. Toward high-efficient red emissive carbon dots: facile preparation, unique properties, and applications as multifunctional theranostic agents. *Chem Mater*. 2016;28:8659–68.
- Miao X, Yan X, Qu D, Li D, Tao FF, Sun Z. Red emissive sulfur, nitrogen codoped carbon dots and their application in ion detection and theranostics. *ACS Appl Mater Interfaces*. 2017;9:18549–56.
- Light WR, Olson JS. Transmembrane movement of heme. *J Biol Chem*. 1990;265:15623–31.
- Hargrove MS, Whitaker T, Olson JS, Vali RJ, Mathews AJ. Quaternary structure regulates heme dissociation from human hemoglobin. *J Biol Chem*. 1997;272:17385–9.
- Aich A, Pan W, Vekilov PG. Thermodynamic mechanism of free heme action on sickle cell hemoglobin polymerization. *AIChE J*. 2015;61:2861–70.
- Levin G, Cogan U, Levy Y, Mokady S. Riboflavin deficiency and the function and fluidity of rat erythrocyte-membranes. *J Nutr*. 1990;120:857–61.
- Goldstein L, Teng ZP, Zeserson E, Patel M, Regan RF. Heme induces an iron-dependent, oxidative injury to human neuron-like cells. *J Neurosci Res*. 2003;73:113–21.
- Chou AC, Fitch CD. Hemolysis of mouse erythrocytes by ferriprotoporphyrin IX and chloroquine. Chemotherapeutic implications. *J Clin Invest*. 1980;66:856–8.
- Kuross SA, Rank BH, Hebbel RP. Excess heme in sickle erythrocyte inside-out membranes: possible role in thiol oxidation. *Blood*. 1988;71:876–82.
- Dutra FF, Alves LS, Rodrigues D, Fernandez PL, Oliveira RB, Golenbock DT, et al. Hemolysis-induced lethality involves inflammasome activation by heme. *Proc Natl Acad Sci U S A*. 2014;111:E4110–8.
- Buehler PW, D'Agostino F. Toxicological consequences of extracellular hemoglobin: biochemical and physiological perspectives. *Antioxid Redox Signal*. 2010;12:275–91.
- Kumar S, Bandyopadhyay U. Free heme toxicity and its detoxification systems in human. *Toxicol Lett*. 2005;157:175–88.
- Huy NT, Dai TXT, Uyen DT, Sasai M, Harada S, Kamei K. An improved colorimetric method for quantitation of heme using tetramethylbenzidine as substrate. *Anal Biochem*. 2005;344:289–91.
- Crouser ED, Gadd ME, Julian MW, Huff JE, Broekemeier KM, Robbins KA, et al. Quantitation of cytochrome *c* release from rat liver mitochondria. *Anal Biochem*. 2003;317:67–75.
- Luo D, Huang J. Determination of cytochrome *c* and other heme proteins using the reduction wave of mercury protoporphyrin IX groups generated by a hydroxylamine induced replacement reaction. *Anal Chem*. 2009;81:2032–6.
- Liu SC, Zhai S, Palek J. Detection of heme release during hemoglobin S denaturation. *Blood*. 1988;71:1755–8.
- Mehta VN, Jha S, Basu H, Singhal RK, Kailasa SK. One-step hydrothermal approach to fabricate carbon dots from apple juice for imaging of mycobacterium and fungal cells. *Sensors Actuators B Chem*. 2015;213:434–43.
- Yang Q, Wei L, Zheng X, Xiao L. Single particle dynamic imaging and Fe<sup>3+</sup> sensing with bright carbon dots derived from bovine serum albumin proteins. *Sci Rep*. 2015;5:17727.
- Ji L, Chen L, Wu P, Gervasio DF, Cai C. Highly selective fluorescence determination of the hematin level in human erythrocytes with no need for separation from bulk hemoglobin. *Anal Chem*. 2016;88:3935–44.
- Lu S, Sui L, Liu J, Zhu S, Chen A, Jin M, et al. Near-infrared photoluminescent polymer-carbon nanodots with two-photon fluorescence. *Adv Mater*. 2017;29:1603443.
- Liu J, Li D, Zhang K, Yang M, Sun H, Yang B. One-step hydrothermal synthesis of nitrogen-doped conjugated carbonized polymer dots with 31% efficient red emission for in vivo imaging. *Small*. 2018;17:03919.
- Song W, Duan W, Liu Y, Ye Z, Chen Y, Chen H, et al. Ratiometric detection of intracellular lysine and pH with one-pot synthesized dual emissive carbon dots. *Anal Chem*. 2017;89:13626–33.
- Lan M, Zhao S, Zhang Z, Yan L, Guo L, Niu G, et al. Two-photon-excited near-infrared emissive carbon dots as multifunctional agents for fluorescence imaging and photothermal therapy. *Nano Res*. 2017;10:3113–23.
- Sun X, Bruckner C, Lei Y. One-pot and ultrafast synthesis of nitrogen and phosphorus co-doped carbon dots possessing bright dual wavelength fluorescence emission. *Nanoscale*. 2015;7:17278–82.
- Olgun U, Gülfen M. Doping of poly(o-phenylenediamine): spectroscopy, voltammetry, conductivity and band gap energy. *React Funct Polym*. 2014;77:23–9.
- Lu W, Gong X, Nan M, Liu Y, Shuang S, Dong C. Comparative study for N and S doped carbon dots: synthesis, characterization and applications for Fe<sup>3+</sup> probe and cellular imaging. *Anal Chim Acta*. 2015;898:116–27.
- Qu S, Zhou D, Li D, Ji W, Jing P, Han D, et al. Toward efficient orange emissive carbon nanodots through conjugated sp<sup>2</sup>-domain controlling and surface charges engineering. *Adv Mater*. 2016;28:3516–21.
- Ananthanarayanan A, Wang Y, Routh P, Sk MA, Than A, Lin M, et al. Nitrogen and phosphorus co-doped graphene quantum dots: synthesis from adenosine triphosphate, optical properties, and cellular imaging. *Nanoscale*. 2015;7:8159–65.



37. Nie H, Li M, Li Q, Liang S, Tan Y, Sheng L, et al. Carbon dots with continuously tunable full-color emission and their application in ratiometric pH sensing. *Chem Mater*. 2014;26:3104–12.
38. Liu J, Lu S, Tang Q, Zhang K, Yu W, Sun H, et al. One-step hydrothermal synthesis of photoluminescent carbon nanodots with selective antibacterial activity against *Porphyromonas gingivalis*. *Nanoscale*. 2017;9:7135–42.
39. Yuan F, Ding L, Li Y, Li X, Fan L, Zhou S, et al. Multicolor fluorescent graphene quantum dots colorimetrically responsive to all-pH and a wide temperature range. *Nanoscale*. 2015;7:11727–33.
40. Wu X, Song Y, Yan X, Zhu C, Ma Y, Du D, et al. Carbon quantum dots as fluorescence resonance energy transfer sensors for organophosphate pesticides determination. *Biosens Bioelectron*. 2017;94:292–7.
41. Zhang QQ, Chen BB, Zou HY, Li YF, Huang CZ. Inner filter with carbon quantum dots: a selective sensing platform for detection of hematin in human red cells. *Biosens Bioelectron*. 2018;100:148–54.